GL-TR-90-0349

AD–A237 675

║█║██║█║██║█║█║██║█║█║█║

Effects of Solar Heating by Aerosols
and Trace Gases on the Temperature Structure Constant

J.R. Hummel
E.P. Shettle

SPARTA, Inc.
24 Hartwell Avenue
Lexington, MA 02173

DTIC
ELECTE
JUL 0 8 1991
B

9 August 1990

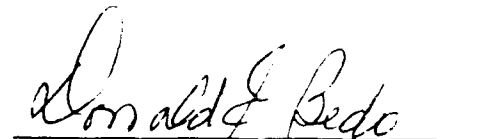Scientific Report No. 6

Approved for Public Release; Distribution Unlimited

GEOPHYSICS LABORATORY
AIR FORCE SYSTEMS COMMAND
UNITED STATES AIR FORCE
HANSCOM AIR FORCE BASE, MASSACHUSETTS 01731-5000

91-03945
║█║██║██║█║█║█║██║█║

"This technical report has been reviewed and approved for publication"

Robert R. Beland
Contract Manager

Donald E. Bedo, Chief
Electro-Optical Measurement Branch

FOR THE COMMANDER

R. Earl Good, SES, Director
Optical Environment Division

REPORT DOCUMENTATION PAGE

1a. REPORT SECURITY CLASSIFICATION	1b. RESTRICTIVE MARKINGS
UNCLASSIFIED	

2a. SECURITY CLASSIFICATION AUTHORITY	3. DISTRIBUTION / AVAILABILITY OF REPORT
	APPROVED FOR PUBLIC RELEASE;
2b. DECLASSIFICATION / DOWNGRADING SCHEDULE	DISTRIBUTION UNLIMITED

4. PERFORMING ORGANIZATION REPORT NUMBER(S)	5. MONITORING ORGANIZATION REPORT NUMBER(S)
LTR90-009	GL-TR-90-0349

6a. NAME OF PERFORMING ORGANIZATION	6b. OFFICE SYMBOL (If applicable)	7a. NAME OF MONITORING ORGANIZATION
SPARTA, INC.		GEOPHYSICS LABORATORY

6c. ADDRESS (City, State, and Zip Code)	7b. ADDRESS (City, State, and Zip Code)
24 HARTWELL AVENUE LEXINGTON, MA 02173	HANSCOM AFB, MA 01731-5000

8a. NAME OF FUNDING / SPONSORING ORGANIZATION	8b. OFFICE SYMBOL (If applicable)	9. PROCUREMENT INSTRUMENT IDENTIFICATION NUMBER
		F19628-88-C-0038

8c. ADDRESS (City, State, and Zip Code)	10. SOURCE OF FUNDING NUMBERS			
	PROGRAM ELEMENT NO.	PROJECT NO.	TASK NO.	WORK UNIT ACCESSION NO.
	62101F	7670	15	AP

11. TITLE (Include Security Classification)

EFFECTS OF SOLAR HEATING BY AEROSOLS AND TRACE GASES ON THE TEMPERATURE STRUCTURE CONSTANT

12. PERSONAL AUTHOR(S)

J. R. Hummel and E. P. Shettle*

13. TYPE OF REPORT	13b. TIME COVERED		14. DATE OF REPORT (Year, Month, Day)	15. PAGE COUNT
SCIENTIFIC REPORT #6	FROM 07/01/88	TO 12/31/90	1990 AUGUST 9	24

16. SUPPLEMENTARY NOTATION

*Naval Research Laboratory, Code 65221
Washington, DC 20375

17.	COSATI CODES		18. SUBJECT TERMS (Continue on reverse if necessary and identify by block number)
FIELD	GROUP	SUB-GROUP	Optical Turbulence, Solar Heating, Ozone, Aerosols, Index of Refraction, Structure Function

19. ABSTRACT (Continue on reverse if necessary and identify by block number)

Thermosonde measurements made in the stratosphere indicate an increase in the temperature structure constant, C_T^2 during daylight hours. Simplified calculations indicate that temperature perturbations resulting from solar heating by thin layers of areosols and ozone could provide the mechanism for the observed day-night differences in C_T^2.

Estimates of the vertical variations in ozone and aerosol abundances on spatial scales between a few tens of meters to about a kilometer have been used with mean ozone and aerosol profiles to make detailed calculations of the solar heating rates by ozone and aerosols. The calculations have utilized the temperature dependent ozone absorption cross sections and the aerosol properties from the AFGL model atmospheres. Perturbations of various amounts and at different altitudes have been applied to the mean ozone and aerosol profiles to study the impact on the heating rates with the goal of trying to understand the stratospheric thermosonde measurements.

20. DISTRIBUTION / AVAILABILITY OF ABSTRACT	21. ABSTRACT SECURITY CLASSIFICATION
☐ UNCLASSIFIED/UNLIMITED ☒ SAME AS RPT. ☐ DTIC USERS	UNCLASSIFIED

22a. NAME OF RESPONSIBLE INDIVIDUAL	22b. TELEPHONE (Include Area Code)	22c. OFFICE SYMBOL
ROBERT BELAND	(617) 377-4604	GL/OPA

DD FORM 1473, 84 MAR

83 APR edition may be used until exhausted
All other editions are obsolete.

Contents

v

Acknowledgement

EFFECTS OF SOLAR HEATING BY AEROSOLS AND TRACE GASES ON THE TEMPERATURE STRUCTURE CONSTANT

1. INTRODUCTION

1.1 Background and Purpose of the Study

The propagation of radiation through the atmosphere can be affected by variations in the index of refraction. These variations can be studied by measuring the index of refraction structure constant, C_n^2. The index of refraction structure constant is a measure of the variations in the atmospheric index of refraction as a function of altitude and, in turn, is a measure of the amount of optical turbulence present in the atmosphere.

Thermosonde measurements of C_n^2 made during daylight conditions indicate an enhancement in the temperature structure constant relative to measurements made at night. Simplified calculations indicate that temperature perturbations resulting from solar heating by aerosols and ozone could provide the mechanism for the observed day-night differences in C_n^2. The purpose of this study is to perform detailed calculations of the solar heating rates of ozone and aerosols on spatial and temporal scales appropriate to the observed variations in the temperature structure constant.

1.2 Organization of Report

Chapter 2 sets the background for the phenomenon, presents some relevant observations, and discusses related studies from the scientific literature. Chapter 3

describes the methodology used to perform the calculations and Chapter 4 discusses the results from the calculations. Finally, Chapter 5 provides the conclusions and recommendations for additional work.

2. BACKGROUND AND RELEVANT OBSERVATIONS

2.1 Background

The Air Force Geophysics Laboratory (AFGL) has undertaken an extensive measurement program of C_n^2 over the years utilizing balloon-borne thermosondes. Thermosondes measure the temperature difference over a one meter horizontal path.[1] The mean square temperature fluctuation is evaluated and over the one meter distance equals the temperature structure constant, C_T^2. The temperature structure constant is then related to the index of refraction structure constant via the relationship, neglecting the small contribution from H_2O,

$$C_n^2(z) = \left[\frac{79.9 P(z) \times 10^{-6}}{T^2(z)} \right]^2 C_T^2(z)$$

where z is the altitude in km, P is the atmospheric pressure in mb, and T is the atmospheric temperature in K. The thermosonde unit is carried piggyback fashion with a conventional radiosonde which measures the pressure, temperature, relative humidity, and wind speed and direction.

The AFGL program has measured C_n^2 at different latitudes and under day and night conditions. The thermosonde measurements of C_n^2 have indicated a dramatic difference between the averaged day and night conditions. Between about 15 and 30 km, there is an enhancement of daytime C_n^2 values that is not seen in the nighttime values. Figure 1 demonstrates the daytime enhancement in C_n^2 by comparing two thermosonde flights taken during a measurement program conducted at Penn State in 1986. The two thermosonde missions were taken on the same day and under the same synoptic weather conditions.

This enhancement is believed to be real and not due to any instrumental effects. One possible explanation for the daytime enhancement is from solar heating by atmospheric gases, such as ozone, and/or aerosols. A detailed examination of possible instrumental sources of error has not indicated an instrumental source for the observed phenomenon.[2] GL is continuing to study the possibility of balloon thermal wake effects on the turbulence measurements. A series of dropsonde tests

---

[1] Brown, J. H., Good, R. E., Bench, P. M., and Faucher, G., (1982) "Sonde Experiments for Comparative Measurements of Optical Turbulence", AFGL-TR-82-0079, ADA 118740, 24 February 1982.

[2] Brown, J. H., Dewan, E., Thomas, P., and Murphy, E., (1989) "Study of Possible Solar Heating Effects on Thermosonde Probes - Error Analysis", Geophysics Laboratory, Hanscom AFB, MA, GL-TR-89-0178, 10 July 1989, ADA 218116.

are planned for late 1990 to study if balloon wake effects could be contributing to the enhancement. The fact that this phenomenon is observed independently of location supports the belief of a solar heating-driven mechanism.

Averaged Thermosonde Data
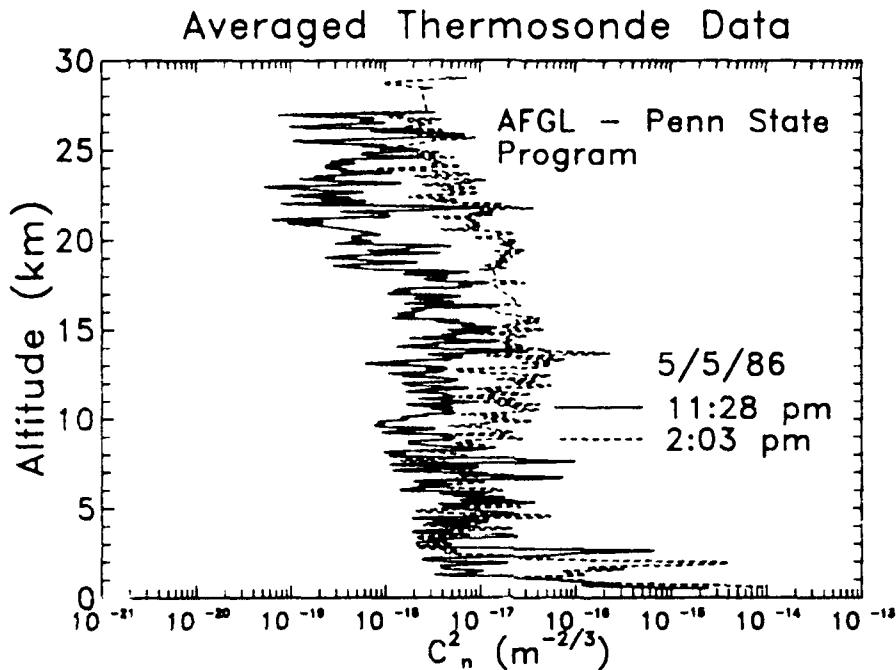
Figure 1. An Example of the Daytime Enhancement in C_n^2 as Measured With an AFGL Thermosonde

2.2 Relevant Observations

Two pieces of observational evidence support the hypothesis that solar heating is the driving force. One, the ozone mixing ratio and solar heating rates are increasing in this altitude range. Also, stratospheric aerosols peak in this altitude range. Second, measurements have shown that the profiles of ozone and stratospheric aerosols exhibit structure on spatial scales small enough to possibly give rise to the thermal variation that ultimately gives rise to the variation in the temperature structure constant.

2.2.1 Ozone Measurements

The vertical profile of ozone is routinely measured using balloon-borne electrochemical ozonesondes, rocketsondes, in situ ultraviolet absorption photometers,

and satellites[3,4,5] These techniques indicate that structure exists in the vertical ozone profile.

Measurements from a balloon-borne high resolution system developed by researchers at Harvard University demonstrate that the ozone mixing ratio varies on a spatial scale consistent with that of the C_n^2 data. Figures 2(a.) and (b.) show a profile of ozone mass mixing ratio measured by the Harvard instrument. The data were obtained over Palestine, Texas at the end of March 1984. Figure 2 (a.) shows the profile over the 15 to 30 km region and Figure 2 (b.) shows the structure in the profile over a selected 2 km region. Figure 2 (a.) also shows the AFGL midlatitude ozone profile for comparison purposes.[6] The data shown in the Figure exhibit a structure in the ozone mass mixing ratio on the order of tens of meters.

2.2.2 Aerosol Measurements

The vertical profile of aerosols in the stratosphere is routinely measured by lidar systems, balloon-borne dustsondes, and satellites (eg.[7]) These measurement systems also demonstrate that structure exists in the aerosol profile. In the case of lidar and dustsonde systems, structure on the order of 100's of meters can be resolved. Figure 3 shows dustsonde measurements of aerosol concentration in the stratosphere for particles with radii greater than $0.15 \mu m$.[8] The results shown in the Figure were taken prior to the eruption of El Chichon and while some of the structure displayed is possibly noise, the data still exhibit the fine structure that is characteristic of aerosol layers.

[3] Dutsch, H.U., and Ling, Ch. (1969) Critical Comparison of the Determination of Vertical Ozone Distribution by the Umkehr Method and by the Electrochemical Sonde, Ann. Geophys., 25:211-214.

[4] McCormick, M.P., Swissler, T.J., Hilsenrath, E., Krueger, A.J., and Osborn, M.T. (1984) Satellite and Correlative Measurements of Stratospheric Ozone: Comparison of Measurements Made by SAGE, ECC Balloons, Chemiluminescent, and Optical Rocketsondes, J. Geophys. Res., 89. 5315-5320.

[5] Hilsenrath, E., Attmannspacher, W., Bass, A., Evans, W., Hagemeyer, R., Barnes, R.A., Komhyr, W., Mauersberger, K., Mentall, J., Profitt, M., Robbins, D., Taylor, S., Torres, A., and Weinstock, E., (1986) Results From the Balloon Ozone Intercomparison Campaign (BOIC), J. Geophys. Res., 91:13137-13152.

[6] Anderson, G.P., Clough, S.A., Kneizys, F.X., Chetwynd, J.H., and Shettle, E.P., (1986) "AFGL Atmospheric Constituent Profiles (0-120 km)", AFGL-TR-86-0110, ADA 175173, 15 May 1986

[7] Hummel, J.R., Shettle, E.P., and Longtin, D.R. (1988) "A New Background Stratospheric Aerosol Model for Use in Atmospheric Radiation Models", Air Force Geophysics Laboratory, Hanscom AFB, MA, AFGL-TR-88-0166, ADA 210110.

[8] Hofmann, D.J., and Rosen, J.M., (1983) "Study of Large Aerosol Particles", University of Wyoming, Laramie, WY, Report # AP-75.
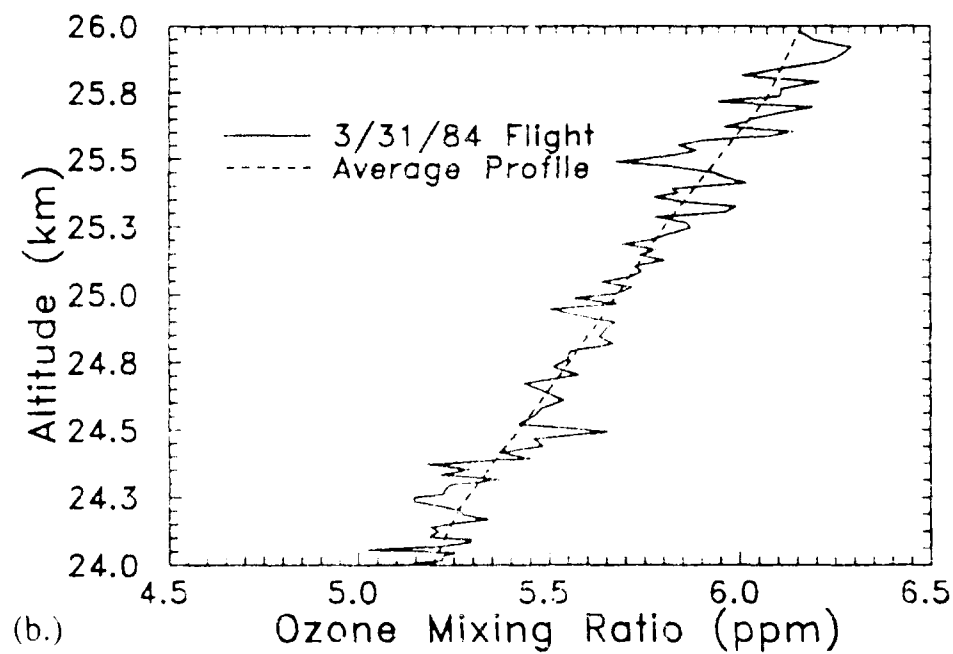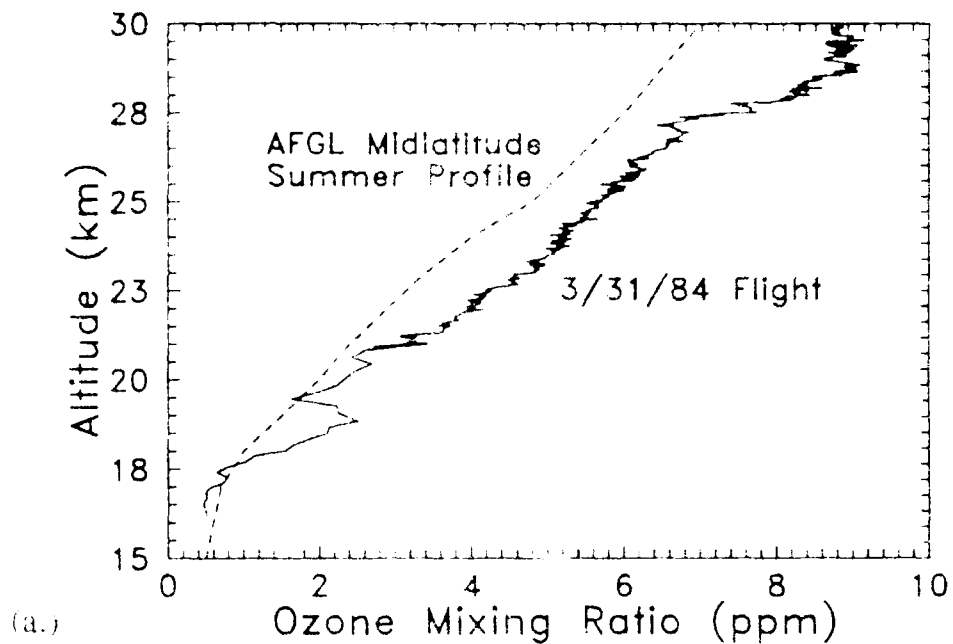
Figure 2. Balloon Measurements of Ozone Mixing Ratio Over (a.) 15 to 30 km and (b.) 24 - 26 km From March 1984. (Data Courtesy of Dr. E. Weinstock, Harvard University.)
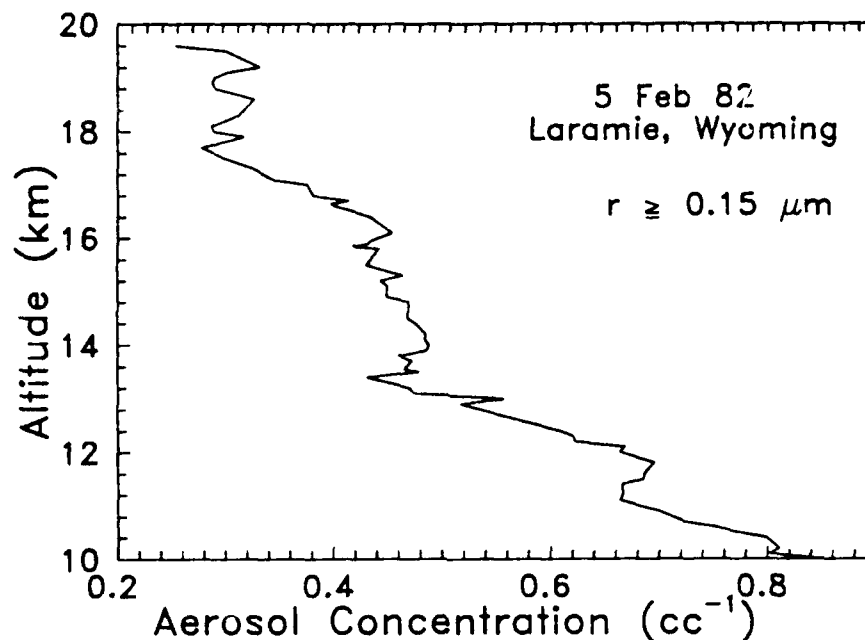
Figure 3. Dustsonde Measurements of Aerosol Concentration as a Function of Altitude

2.3 Related Studies

Fiocco *et Al.*[9,10] have studied the energy exchange that occurs with aerosols in the atmosphere. Their studies have indicated that during daylight hours aerosols can achieve temperatures that differ from the ambient atmosphere. In the upper atmosphere, the solar heated aerosols do not transfer all of the heat energy to the ambient atmosphere, thereby leading to the large aerosol-atmosphere temperature differences. For altitudes below 50 km, the aerosols and atmosphere exchange energy more efficiently. As a result, the difference between the aerosol temperatures and the ambient atmosphere is less than a degree K and is a function of particle size. The larger the particle, the greater the temperature difference.

3. DETAILS OF CALCULATIONS

Calculations were performed for a model atmosphere extending from the surface to 35 km. The atmospheric structure was based on the AFGL midlatitude summer atmosphere.[6] The model atmosphere was divided into 139 layers. The layers

[9] Fiocco, G., Grams, G., and Visconti, V., (1975) Equilibrium Temperatures of Small Particles in the Earth's Upper Atmosphere (50-110 km), *J. Atmos. Terr. Phys.*, 37:1327-1337

[10] Fiocco, G., Grams, G., and Mugnai, A. (1976) Energy Exchange and Temperature of Aerosols in the Earth's Atmosphere (0 - 60 km), *J. Atmos. Sci.*, 33:2415-2424.

were approximately 125 m thick between 15 - 30 km and about 1000 m thick elsewhere. Two layers were combined to form an atmospheric slab, the center of which is where the heating rates were calculated.

Aerosols were introduced at all altitudes. The type and amount of aerosol was assumed to be a function of altitude. The aerosol attenuation properties were based on those used in the AFGL model atmospheres.[11,12] Between 0 - 2 km, rural aerosols based on a relative humidity of 70 % were assumed. In the free troposphere (2 - 10 km), tropospheric aerosols were assumed. Finally, above 10 km, stratospheric aerosols were assumed. Spring/summer conditions were assumed. The type of aerosol, however, was varied in order to study the sensitivity of the calculations on aerosol attenuation properties.

A total of 106 spectral intervals between 0.135 - 0.755 μm were used for the ozone and molecular oxygen calculations. The solar fluxes were based on those used in LOWTRAN 7[13]. The cross sections used were those from LOWTRAN 7 and FASCOD[14,15] The ozone cross section are temperature dependent[16] although the effect of the temperature dependence is negligible.

The aerosol attenuation was calculated over 15 wavelengths between 0.2 - 20 μm. The overlap between the aerosols and gases is also taken into account. For the results discussed in this paper, the calculations where performed for solar noon conditions at equinox. Also, it is assumed that the underlying surface has a surface albedo of 30 %.

[11] Shettle, E. P., and Fenn, R.W. (1979) "Models of the Aerosols of the Lower Atmosphere and the Effects of Humidity Variations", AFGL-TR-79-0214, ADA 08591

[12] Fenn, R.W., Clough, S.A., Gallery, W.O., Good, R.E., Kneizys, F.X., Mill, J.D., Rothman, L.S., Shettle, E.P., Volz, F.E., (1985)"Optical and Infrared Properties of the Atmosphere", Chapter 18 in Handbook of Geophysics and the Space Environment, A.S. Jursa Scientific Editor, Air Force Geophysics Laboratory, Hanscom AFB, MA, AFGL-TR-85-0315, ADA 167000.

[13] Kneizys, F.X., Shettle, E.P., Abreu, L.W., Chetwynd, J. H., Anderson, G.P., Gallery, W.O., Selby, J.E.A, and Clough, S.A., (1988) "Users Guide to LOWTRAN 7", AFGL-TR-88-0177, ADA 206773, 16 August 1988.

[14] Clough, S.A., Kneizys, F.X., Shettle, E.P., and Anderson, G.P. (1986) "Atmospheric Radiance and Transmittance: FASCODE 2", Proc. of the Sixth Conference on Atmospheric Radiation, Williamsburg, VA, American Meteorological Society, Boston, MA.

[15] Clough, S.A., Kneizys, F.X., Anderson, G.P., Shettle, E.P., Chetwynd, J.H., Hall, L.A., and Worsham, R.D. (1989) "FASCOD 3: Spectral Simulations", IRS 88: Current Problems in Atmospheric Radiation, Proceedings, J. Lenoble and J.F. Geleyn, Ed., A. Deepak Publishing, Hampton, VA, 372-375.

[16] Anderson, G.P., Kneizys, F.X., Shettle, E.P., Abreu. L.W., Chetwynd, J.H., Huffman, R.E., and Hall, L.A., (1990) Spectral Simulations in the UV, submitted to Appl. Optics.

4. RESULTS

4.1 Unperturbed Conditions

Figure 4 shows the calculated solar heating rates for the assumed unperturbed atmospheric conditions. The solid curve is the solar heating rate from ozone, molecular oxygen and aerosols. The curve marked "Gases only" is the calculated solar heating rate if aerosols were not present. The calculations assumed a stratospheric aerosol profile appropriate for background conditions but with attenuation properties representative of aged volcanic aerosols. Aged volcanic aerosols are considerably more absorbing than background stratospheric aerosols and these results give a feel for the relative role of stratospheric aerosols in determining the stratospheric solar heating rates. These calculations demonstrate the apparent insensitivity of the total solar heating rate to background stratospheric aerosols. It should be stressed, however, that these calculations are representative of background stratospheric conditions.
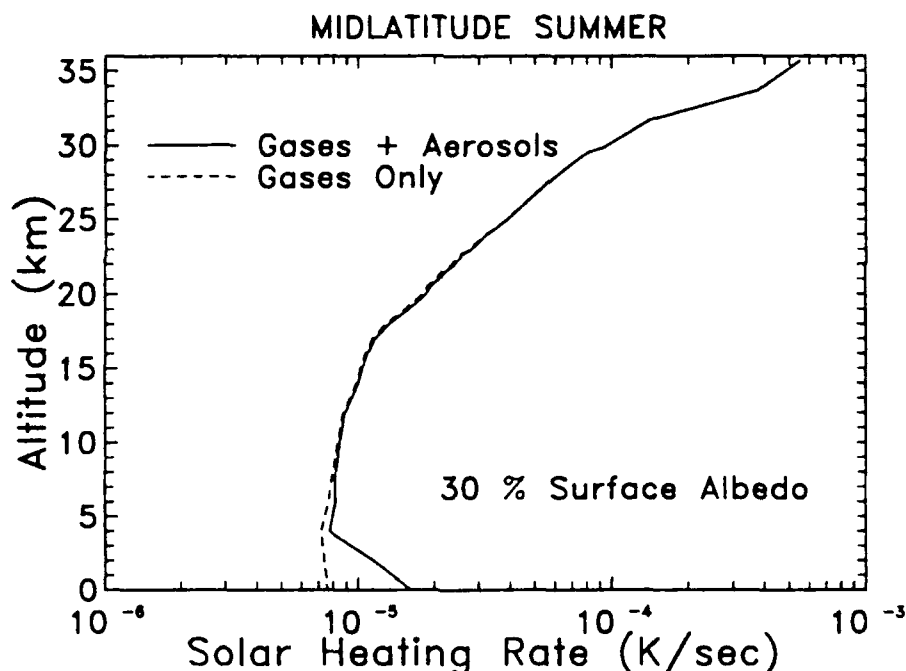
Figure 4. Calculated Solar Heating Rates for the Background, Unperturbed Model Atmosphere

4.2 Perturbed Conditions

Figure 5 displays heating rates for the model atmosphere with perturbations in the (a.) aerosol and (b.) ozone concentrations. In both cases it is assumed that the perturbation occurs over a 20 m layer centered at 25 km and that the peak-to-peak perturbation is 50% of the mean concentrations.

8

Figure 5. Heating Rate as a Function of Altitude Assuming a 50 % Change in (a.) the Aerosol and (b.) Ozone Concentrations

4.3 Determining the Solar Heating Rates Required to Initiate Turbulence

Turbulence is initiated when the local Richardson number, Ri, is less than the critical Richardson number, $1/4$. The local Richardson number is given as the ratio of the bouyancy to shear as

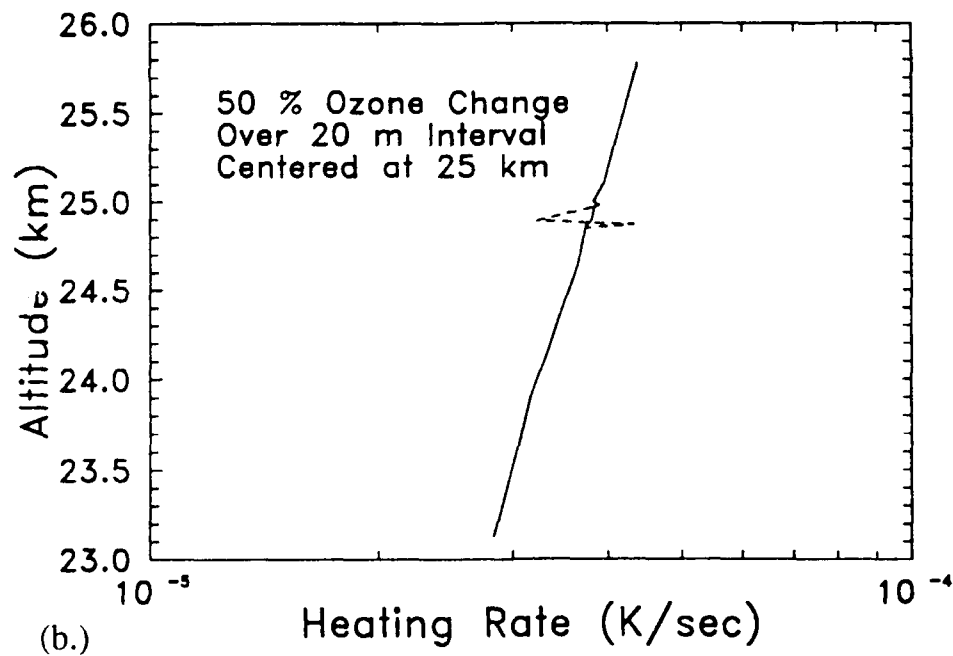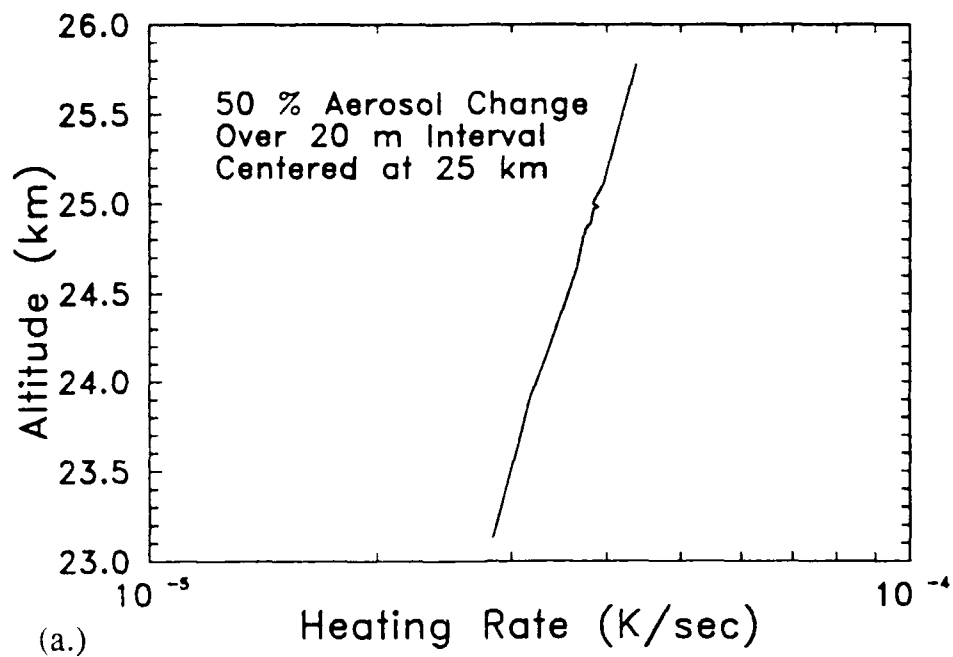$$Ri = \frac{g}{TS^2}\left(\frac{\partial T}{\partial z} + \gamma_a\right) \tag{1}$$

g is the acceleration of gravity, T is the temperature in K, S is the local vertical wind shear, $\frac{\partial T}{\partial z}$ is the local vertical gradient in temperature, and γ_a is the adiabatic lapse rate, 0.0098 K/m. For instability to occur, (1) is expressed as

$$1/4 > \frac{g}{TS^2}\left(\frac{\partial T}{\partial z} + \gamma_a\right) \tag{2}$$

Solving (2) for the temperature gradient required for instability to occur, one can solve for the critical temperature gradient $\left(\frac{\partial T}{\partial z}\right)_c$

$$\left(\frac{\partial T}{\partial z}\right)_c = \frac{TS^2}{4g} - \gamma_a$$

For representative stratospheric temperatures, Figure 6 displays the values of critical lapse rate as a function of wind shear. Lapse rates to the right of the curves represent regions of instability and possible turbulence onset.
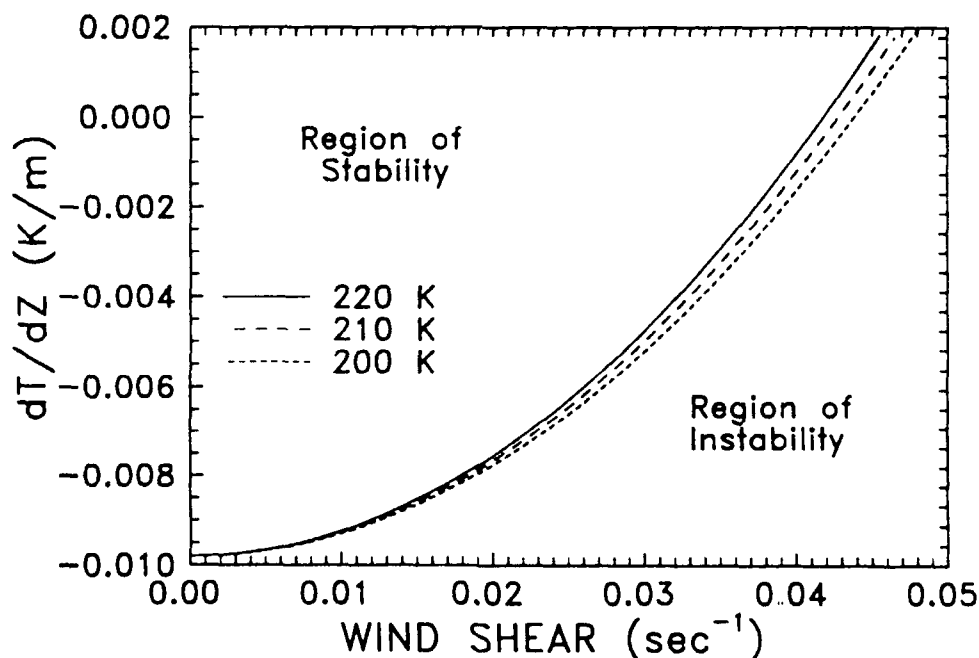

Figure 6. Values of the Critical Temperature Gradient as a Function of Wind Shear for Three Representative Stratospheric Temperatures

10

In order to induce turbulence, the layers of ozone and aerosol must persist long enough to produce a lapse rate over the layer that exceeds the critical value. Layers on the order of 25 m can persist for as long as 12 to 43 minutes, depending upon the degree of layer spreading.

If an aerosol layer 20 m thick existed with a 50 % peak-to-peak perturbation in the concentration, the resulting difference in solar heating rate (relative to the unperturbed values) would be 1.5×10^{-8} K s^{-1} m^{-1}. If this layer persisted for 45 minutes, the $\frac{\partial T}{\partial z}$ would amount to 4.0×10^{-5} K m^{-1}. In order for turbulence to begin, an unrealistically large wind shear would be required. This result indicates that it is unlikely that perturbations in the background stratospheric aerosol abundances are responsible for the enhancement seen in C_n^2.

For an ozone layer 20 m thick with a 50 % peak-to-peak perturbation in the concentration, the resulting difference in solar heating rate is -1.6×10^{-6} K s^{-1} m^{-1}. If this layer persisted for 45 minutes, the $\frac{\partial T}{\partial z}$ would amount to -4.4×10^{-3} K m^{-1}.

In order to induce turbulence in the presence of the above perturbation, wind shears on the order of about 0.03 s^{-1} or greater would be required. Stratospheric wind shears measured during the Penn State program routinely exceeded this value, as shown in Figure 7. This provides support to the hypothesis that solar heating by the ozone layers could be inducing turbulence.

4.4 Sensitivity of Results to Model Calculations

4.4.1 Impact of Local Time

The discussion above was based on results obtained at local noon. Figure 8 presents the heating rate gradient, $\frac{\partial}{\partial z}\left(\frac{\partial T}{\partial t}\right)$, as a function of local time. The results are given for two surface albedo conditions, an ozone perturbation of 50%, and a midlatitude atmosphere.

The heating rate gradient decreases as the local time increases up to local noon, after which it increases. The variation in heating rate gradient is due to changes in the solar zenith angle and corresponding changes in mass path. Such variation is consistent with changes in C_n^2 with solar zenith angle as discussed in Reference 2.

4.4.2 Impact of Latitude

The discussion above was based on results obtained for a latitude of 45° N. Calculations were performed for conditions at 35° N and yielded small increase in the heating rate gradient of 16 % relative to those at 45°. The slight increase is due to the larger amounts of stratospheric ozone present at the lower latitude[12] and is consistent with thermosonde measurement variations with latitude.
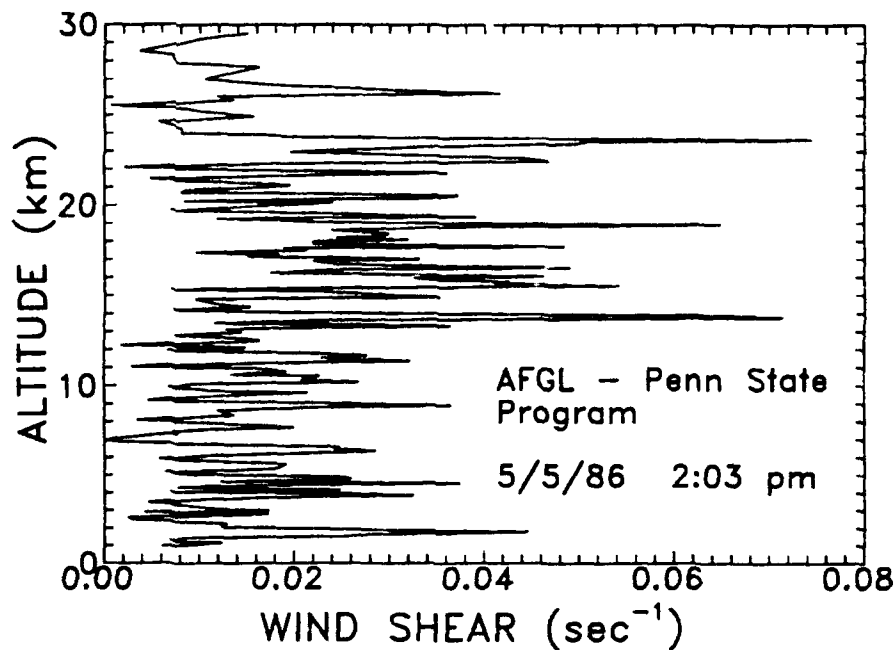
11

Figure 7. An Example of Vertical Wind Shears Measured During the AFGL - Penn State Measurement Program. The data shown were obtained at an altitude resolution of about 250 m
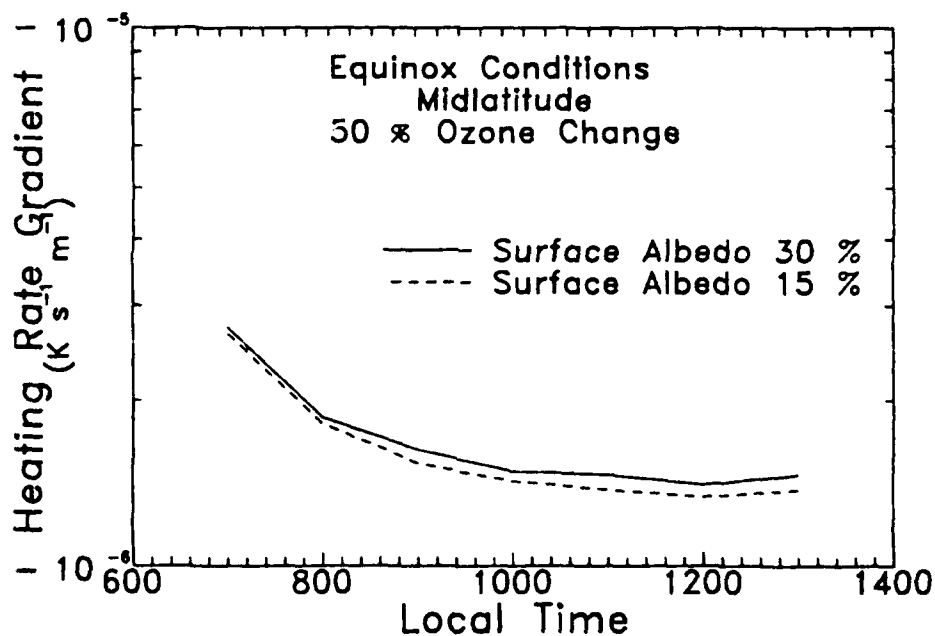

Figure 8. Heating Rate Gradient as a Function of Local Time for Two Different Solar Albedo Conditions

12

4.4.3 Impact of the Height of Perturbation

The height where the perturbation occurs will have an impact on the results of the calculations. This is due to the fact that both the ozone and aerosol profiles are changing in the stratosphere. The ozone mixing ratio profile is increasing in the altitude range where the C_n^2 enhancements are observed. Also, the stratospheric extinction coefficient profile peaks in the 10 - 20 km region, the peak altitude depending on the degree of volcanic activity.

If the ozone perturbation was assumed to occur at 20 km rather than 25 km, the resultant heating rate gradient is lowered by over a factor of three to -4.8×10^{-7} K s^{-1} m^{-1}. If the aerosol perturbation occurred at 20 km, the increase in heating rate gradient is negligible.

4.4.4 Impact of Choice of Stratospheric Aerosol

Calculations were done using an aerosol profile representative of fresh and aged aerosols under extreme volcanic conditions.[12] The calculations were performed with an assumed 50% perturbation over a 20 m interval centered at 20 and 25 km.

With fresh volcanic aerosols and the perturbation centered at 20 km the heating rate gradient is about -3×10^{-6} K s^{-1} m^{-1}. This is 5 - 6 times larger than the heating rate gradient due to a perturbation in the ozone abundance at this altitude. With the perturbation centered at 25 km the heating rate is -3×10^{-7} K s^{-1} m^{-1}.

When aged aerosols are present, the resultant heating rate gradient for a 50% perturbation in the aerosols over a 20 m interval centered on 25 km was -3.4×10^{-8} K s^{-1} m-1. This is over twice that used for the default conditions but still significantly smaller than for ozone perturbations. If the perturbation occurred at about 20 km, on the other hand, the altitude where the enhanced volcanic extinction profile is maximum, the resultant heating rate gradient would be -2.8×10^{-6} K s^{-1} m^{-1}. This value is on the order of that found for ozone perturbations.

What these results indicate is that large amounts of volcanic aerosols could lead to heating rate gradients large enough to produce lapse rates that could exceed the critical lapse rates required to produce instabilities. Again, this is consistent with the larger diurnal variations of C_n^2 as measured by the thermosonde in Hawaii where the variations were larger and where daytime values began departing from nighttime values at lower altitudes.

5. SUMMARY AND CONCLUSIONS

5.1 Summary

Thermosonde measurements of C_n^2 made during daylight conditions indicate an enhancement in the temperature structure constant relative to measurements made at night. Simplified calculations indicate that temperature perturbations resulting from solar heating by aerosols and ozone could provide the mechanism for the observed day-night differences in C_n^2. However, no estimates have been made for C_n^2 resulting from this mechanism. rather, the possibility is established for the generation of turbulence.

Two pieces of observational evidence support the hypothesis that solar heating is the driving force. One, the ozone mixing ratio and solar heating rates due to ozone are increasing in this altitude range. Also, stratospheric aerosols peak in this altitude range. Second, measurements have shown that the profiles of ozone and stratospheric aerosols exhibit structure on spatial scales small enough to possibly give rise to the thermal variation that ultimately gives rise to the variation in the temperature structure constant.

5.2 Conclusions

5.2.1 Role of Perturbations in Ozone

The results for assessing the role of perturbations in the ozone solar heating are encouraging. Calculations of lapse rates that would result from solar heating effects alone indicate that layers on the order of 20 m with perturbations in the ozone profile as high as 50 % could give rise to turbulence onset in the stratosphere.

5.2.2 Role of Perturbations in Stratospheric Aerosols

A perturbation of 50% in the background stratospheric aerosol concentration over a 20 m interval centered at 25 km produces a change in solar heating rate on the order of -10^{-8} K s^{-1} m^{-1}, two orders of magnitude smaller than that from a corresponding 50% perturbation in ozone. When the perturbation occurs at 20 km, the heating rate gradient is still on the order of -10^{-8} K s^{-1} m^{-1}. These results indicate that it is unlikely that perturbations in the *background* stratospheric aerosols could be responsible for the observed variations in the temperature structure constant.

When an extreme volcanic aerosol profile is assumed, the heating rate gradient is on the order of -10^{-7} to -10^{-8}K s^{-1} m^{-1}, depending on the type of volcanic aerosols present, for a perturbation occurring at 25 km but is on the order of -10^{-6} K s^{-1} m^{-1} which is on the order of or larger than that from perturbations in the ozone abundance. These results indicate that in the presence of extreme volcanic conditions, perturbations in the aerosol abundances could give rise to the

enhancement in C_n^2.

The results for assessing the role of perturbations in the ozone solar heating are encouraging. Calculations of lapse rates that would result from solar heating effects alone indicate that layers on the order of 20 m with ozone perturbations as high as 50 % could give rise to turbulence onset in the stratosphere. Thermosonde measurements taken in Hawaii at a time when the Kilauea volcano was active are consistent with larger diurnal variations beginning at lower altitudes.

References

1. Brown, J. H., Good, R. E., Bench, P. M., and Faucher, G., (1982) "Sonde Experiments for Comparative Measurements of Optical Turbulence", AFGL-TR-82-0079, ADA 118740, 24 February 1982.

2. Brown, J. H., Dewan, E., Thomas, P., and Murphy, E., (1989) "Study of Possible Solar Heating Effects on Thermosonde Probes - Error Analysis", Geophysics Laboratory, Hanscom AFB, MA, GL-TR-89-0178, 10 July 1989, ADA 218116.

3. Dutsch, H.U., and Ling, Ch. (1969) Critical Comparison of the Determination of Vertical Ozone Distribution by the Umkehr Method and by the Electrochemical Sonde, *Ann. Geophys.*, **25**:211-214.

4. McCormick, M.P., Swissler, T.J., Hilsenrath, E., Krueger, A.J., and Osborn, M.T. (1984) Satellite and Correlative Measurements of Stratospheric Ozone: Comparison of Measurements Made by SAGE, ECC Balloons, Chemiluminescent, and Optical Rocketsondes, *J. Geophys. Res.*, **89**, 5315-5320.

5. Hilsenrath, E., Attmannspacher, W., Bass, A., Evans, W., Hagemeyer, R., Barnes, R.A., Komhyr, W., Mauersberger, K., Mentall, J., Profitt, M., Robbins, D., Taylor, S., Torres, A., and Weinstock, E., (1986) Results From the Balloon Ozone Intercomparison Campaign (BOIC), *J. Geophys. Res.*, **91**:13137-13152.

6. Anderson, G.P., Clough, S.A., Kneizys, F.X., Chetwynd, J.H., and Shettle, E.P., (1986) "AFGL Atmospheric Constituent Profiles (0-120 km)", AFGL-TR-86-0110, ADA 175173, 15 May 1986

7. Hummel, J.R., Shettle, E.P., and Longtin, D.R. (1988) "A New Background Stratospheric Aerosol Model for Use in Atmospheric Radiation Models", Air Force Geophysics Laboratory, Hanscom AFB, MA, AFGL-TR-88-0166, ADA 210110.

8. Hofmann, D.J., and Rosen, J.M., (1983) "Study of Large Aerosol Particles", University of Wyoming, Laramie, WY, Report # AP-75.

9. Fiocco, G., Grams, G., and Visconti, V., (1975) Equilibrium Temperatures of Small Particles in the Earth's Upper Atmosphere (50-110 km), *J. Atmos. Terr. Phys.*, **37**:1327-1337

10. Fiocco, G., Grams, G., and Mugnai, A. (1976) Energy Exchange and Temperature of Aerosols in the Earth's Atmosphere (0 - 60 km), *J. Atmos. Sci.*, **33**:2415-2424.

11. Shettle, E. P., and Fenn, R.W. (1979) "Models of the Aerosols of the Lower Atmosphere and the Effects of Humidity Variations", AFGL-TR-79-0214, ADA 08591

12. Fenn, R.W., Clough, S.A., Gallery, W.O., Good, R.E., Kneizys, F.X., Mill, J.D., Rothman, L.S., Shettle, E.P., Volz, F.E., (1985)"Optical and Infrared Properties

of the Atmosphere", Chapter 18 in Handbook of Geophysics and the Space, Environment, A.S. Jursa Scientific Editor, Air Force Geophysics Laboratory, Hanscom AFB, MA, AFGL-TR-85-0315, ADA 167000.

13. Kneizys, F.X., Shettle, E.P., Abreu, L.W., Chetwynd, J. H., Anderson, G.P., Gallery, W.O., Selby, J.E.A, and Clough, S.A., (1988) "Users Guide to LOW-TRAN 7", AFGL-TR-88-0177, ADA 206773, 16 August 1988.

14. Clough, S.A., Kneizys, F.X., Shettle, E.P., and Anderson, G.P. (1986) "Atmospheric Radiance and Transmittance: FASCODE 2", Proc. of the Sixth Conference on Atmospheric Radiation, Williamsburg, VA, American Meteorological Society, Boston, MA.

15. Clough, S.A., Kneizys, F.X., Anderson, G.P., Shettle, E.P., Chetwynd, J.H., Hall, L.A., and Worsham, R.D. (1989) "FASCOD 3: Spectral Simulations", IRS 88: Current Problems in Atmospheric Radiation, Proceedings, J. Lenoble and J.F. Geleyn, Ed., A. Deepak Publishing, Hampton, VA. 372-375.

16. Anderson, G.P., Kneizys, F.X., Shettle, E.P., Abreu, L.W., Chetwynd, J.H., Huffman, R.E., and Hall, L.A., (1990) Spectral Simulations in the UV, submitted to *Appl. Optics.*